Cavity optomechanics using an optically levitated nanosphere

D.E. Chang,[1] C.A. Regal,[2] S.B. Papp,[2] D.J. Wilson,[2]
J. Ye,[2,3] O.J. Painter,[4] H.J. Kimble,[2] and P. Zoller[2,5]

[1]*Institute for Quantum Information and Center for the Physics of Information, California Institute of Technology, Pasadena, CA 91125*

[2]*Norman Bridge Laboratory of Physics 12-33, California Institute of Technology, Pasadena, CA 91125*

[3]*JILA, NIST, and Department of Physics, University of Colorado, Boulder, CO 80309*

[4]*Department of Applied Physics, California Institute of Technology, Pasadena, CA 91125*

[5]*Institute for Quantum Optics and Quantum Information of the Austrian Academy of Sciences, A-6020 Innsbruck, Austria*

(Dated: October 25, 2018)

Abstract

Recently, remarkable advances have been made in coupling a number of high-Q modes of nano-mechanical systems to high-finesse optical cavities, with the goal of reaching regimes where quantum behavior can be observed and leveraged toward new applications. To reach this regime, the coupling between these systems and their thermal environments must be minimized. Here we propose a novel approach to this problem, in which optically levitating a nano-mechanical system can greatly reduce its thermal contact, while simultaneously eliminating dissipation arising from clamping. Through the long coherence times allowed, this approach potentially opens the door to ground-state cooling and coherent manipulation of a single mesoscopic mechanical system or entanglement generation between spatially separate systems, even in room temperature environments. As an example, we show that these goals should be achievable when the mechanical mode consists of the center-of-mass motion of a levitated nanosphere.

One of the most intriguing questions associated with quantum theory is whether effects such as quantum coherence and entanglement can be observed at mesoscopic or macroscopic scales. As a first step towards resolving this question, recently much effort has been directed toward quantum state preparation of a number of high-Q modes of nano- and micro-mechanical systems – in particular, cooling such systems to their quantum ground state [1]. Reaching a regime where the quantum behavior of mechanical devices emerges is not only of fundamental interest, but could lead to new applications in fields such as ultra-sensitive detection [2] and quantum information science [3]. To reach this regime, it is critical that the thermalization and decoherence rates of these systems be minimized, by reducing the coupling to their thermal reservoirs. Thus far, this has necessitated the use of cryogenic operating environments. From an engineering standpoint, it would also be desirable to reduce the dissipation and thermalization rates of these systems through their clamping and material supports [4], so that these rates might approach their fundamental material limits [5].

Here we propose a novel approach toward this problem, where the material supports are completely eliminated by optically levitating [6] a nano-mechanical system inside a Fabry-Perot optical cavity. Indeed, since the pioneering work of Ashkin on optical trapping of dielectric particles [6] (in the classical domain), it has been realized that levitation under good vacuum conditions can lead to extremely low mechanical damping rates [7, 8]. We show, however, that such an approach should also facilitate the emergence of quantum behavior even in room-temperature environments, when the particles are of sub-wavelength scale such that the effects of optical scattering become negligible. As a specific example, we show that the center-of-mass (CM) motion of a levitated nanosphere can be optically self-cooled [9, 10, 11] to the ground state starting from room temperature. This system constitutes an extreme example of environmental isolation, as the CM motion is naturally decoupled from the internal degrees of freedom in addition to the external isolation provided by levitation. The long coherence time also allows for the preparation of more exotic states through *coherent* quantum evolution. Here, we consider in detail two examples. First, we describe a technique to prepare a squeezed motional state, which can subsequently be mapped onto light leaving the cavity using quantum state transfer protocols [12, 13, 14, 15]. Under realistic conditions, the output light exhibits up to $\sim$15 dB of squeezing relative to vacuum noise levels, potentially making this system a viable alternative to traditional

techniques using nonlinear crystals [16]. Second, we show that entanglement originally shared between two modes of light [17] can be efficiently transferred onto the motion of two spheres trapped in spatially separate cavities, creating well-known Einstein-Podolsky-Rosen (EPR) correlations [18] between the mechanical systems. Our approach of optical levitation mirrors many successful efforts to cool [19, 20], manipulate [21] and entangle [22] the motion of atoms and ions in room-temperature environments. At the same time, our system has a number of potential advantages, in that it enables direct imaging via strong fluorescence, exhibits large trap depths, and has a relatively large mass. We also note recent related experiments involving opto-mechanical "fluids" (with a continuous excitation spectrum rather than discrete modes) in the form of trapped, ultracold atomic gases [23, 24].

Beyond the examples presented here, the use of a levitated device as an opto-mechanical system could open the door to many interesting opportunities. For instance, it should allow mechanical damping to approach fundamental material limits, potentially enabling the exploration of nanoscale material properties. By levitating systems with internal vibrational modes, multiple modes could be optically addressed and cooled. In addition, the CM oscillation frequency can be tuned through the trapping intensity, allowing for adiabatic state transfer [25] with other modes or matching spatially separate systems for optical linking and entanglement generation [26]. Furthermore, this paradigm integrates nano-mechanics with many techniques for atomic trapping and manipulation, which can be further extended by levitating systems containing an internal electronic transition (*e.g.*, a color center within a nano-crystal [27]). Finally, as illustrated by squeezed light generation, engineering mechanical nonlinearities in conjunction with quantum state transfer yields a novel means to realize nonlinear optical processes.

I. OPTICAL FORCES AND NOISE ACTING ON A DIELECTRIC SPHERE

To illustrate our idea, we consider a sub-wavelength dielectric sphere interacting with two standing-wave optical modes of a Fabry-Perot cavity (Fig. 1a). One resonantly driven mode provides an optical dipole trap for the sphere. The second mode is driven by a weaker "cooling" beam, assumed to have a non-zero intensity gradient at the trap center, which provides a radiation pressure cooling force [9, 10, 11]. We discuss the cooling mechanism in the next section, while here we focus on the trapping potential and the noise forces acting

on the sphere.

The trapping beam provides a gradient force similar to that used to "optically tweeze" small dielectric particles [6]. Considering a sphere whose radius is much smaller than the optical wavelength, $r \ll \lambda$, its optical response is like that of a point dipole with induced dipole moment $p_{\rm ind} = \alpha_{\rm ind} E(x)$ and optical potential $U_{\rm opt}(x) = -(1/4)(\mathrm{Re}\ \alpha_{\rm ind})|E(x)|^2$ (see Appendix). Here x is the CM position of the sphere, $\alpha_{\rm ind} = 3\epsilon_0 V \left(\frac{\epsilon-1}{\epsilon+2}\right)$ is its polarizability, V is the sphere volume, and ϵ is the electric permittivity. Taking a standing wave $E(x) = E_0 \cos kx$ ($k \equiv 2\pi/\lambda$), to lowest order near an anti-node the potential corresponds to a harmonic oscillator with mechanical frequency

$$\omega_m = \left(\frac{6k^2 I_0}{\rho c} \mathrm{Re} \frac{\epsilon - 1}{\epsilon + 2} \right)^{1/2}, \tag{1}$$

where I_0 is the field intensity and ρ is the mass density of the sphere. The total trap depth is $U_0 = (3I_0 V/c)\mathrm{Re}\frac{\epsilon-1}{\epsilon+2}$. Typical trap depths and oscillation frequencies for a high-index material ($\frac{\epsilon-1}{\epsilon+2} \sim 1$) are plotted in Figs. 1c,d. Frequencies of several MHz are achievable using an intra-cavity intensity of $I_0 \sim 1$ W/μm^2. The imaginary component of ϵ characterizes optical absorption, which contributes to internal heating. For a material with $\sim$10 dB/km propagation losses in bulk, intensities of $I_0 \sim 10$ W/μm^2 can be sustained without melting the sphere, due to blackbody re-radiation of the absorbed energy (see Appendix). With this in mind, we assume ϵ is real in following discussions.

The dominant noise forces acting on the sphere are collisions with a background gas and momentum recoil kicks due to scattered photons. In the Appendix, we show that the contributions from shot noise, blackbody radiation, and sphere anisotropy are negligible. Furthermore, the CM is de-coupled from the internal degrees of freedom and the sphere effectively has no internal structure (as opposed to molecules, where the internal configuration can affect cooling efficiency [28]). In the regime where the molecular mean free path exceeds r, the background gas leads to a mean damping force $dp/dt = -\gamma_g p/2$ with damping rate $\gamma_g/2 = (8/\pi)(P/\bar{v}r\rho)$, where $P, \bar{v}$ are the background gas pressure and mean speed, respectively [29]. The random nature of the collisions also thermalizes the motional energy, at a rate given through the fluctuation-dissipation theorem by $dE/dt = -\gamma_g(E - k_B T)$, where T is the gas temperature. In particular, the characteristic time for the system to heat by one phonon starting from the ground state is $\tau_g \sim \hbar\omega_m/\gamma_g k_B T$. Note that τ_g^{-1} does not necessarily reflect the actual collision rate between the sphere and gas molecules, $R_{\rm coll} \approx \pi P \bar{v} r^2/k_B T$ (it

is possible for a single collision to be quite rare, $R_{\rm coll} \gg \tau_g^{-1}$, and to impart several phonons at once). We define a mechanical quality factor $Q_g = \omega_m/\gamma_g$ due to the background gas, and a number of coherent oscillations $N_{\rm osc}^{(g)} \equiv \omega_m \tau_g / 2\pi$ expected before the energy increases by a single phonon. For a sphere of radius $r = 50$ nm, $\omega_m/(2\pi) = 1$ MHz, and a room-temperature gas with $P = 10^{-10}$ Torr, one finds $\gamma_g \sim 10^{-6}$ s^{-1}, $Q_g \sim 6\times10^{12}$, $N_{\rm osc}^{(g)} \sim 10^5$, indicating that the levitated sphere can be essentially *de-coupled* from its thermal environment.

Photons scattered by the sphere out of the cavity lead to heating via momentum recoil kicks. In analogy with atoms or ions trapped in the Lamb-Dicke regime [21] (when the particle is trapped on a scale Δx much smaller than λ), the scattering induces transitions between consecutive harmonic oscillator levels $n \to n \pm 1$, with rates $R_{n\to n\pm1} = \gamma_{\rm sc}(n + 1/2 \pm 1/2)$. Second-order perturbation theory [30] yields

$$\gamma_{\rm sc} = (2/5)(\omega_r/\omega_m) R_{\rm sc}, \tag{2}$$

where $\omega_r = \hbar k^2/2\rho V$ is the recoil frequency and $R_{\rm sc} = 48\pi^3 \frac{I_0 V^2}{\lambda^4 \hbar \omega} (\frac{\epsilon-1}{\epsilon+2})^2$ is the photon scattering rate. A result identical to Eq. (2) holds for a weakly excited, trapped atom [31]. When photon scattering dominates the heating, the expected number of coherent oscillations is

$$N_{\rm osc}^{(\rm sc)} \equiv \frac{\omega_m}{2\pi\gamma_{\rm sc}} = \frac{5}{8\pi^3} \frac{\epsilon+2}{\epsilon-1} \frac{\lambda^3}{V}. \tag{3}$$

Note that $N_{\rm osc}^{(\rm sc)}$ scales inversely with the sphere volume ($N_{\rm osc}^{(\rm sc)} \sim 40$ for $r = 50$ nm, $\lambda = 1$ μm, $\epsilon \gg 1$), due to the fact that the scattered power and dipole force scale like $p_{\rm ind}^2$ and $p_{\rm ind}$, respectively. Comparing with background gas collisions at $P = 10^{-10}$ Torr and $\omega_m/(2\pi) = 1$ MHz, recoil heating dominates $N_{\rm osc}$ for sphere sizes $r \gtrsim 5$ nm. Reaching the regime $N_{\rm osc} \gg 1$ implies that the sphere can coherently evolve for many oscillation periods after any cooling mechanisms are turned off, which makes this system a promising candidate for observing coherent quantum phenomena.

Finally, we remark that $R_{\rm sc}$ can be very large ($R_{\rm sc} \sim 10^{15}$ s^{-1} for $I_0 = 1$ W/μm^2 and $r = 50$ nm) compared to atoms or ions, which enables direct imaging. The large scattering is due to the large intensities and the linear response of the sphere (it is not saturated like an atom or ion), as opposed to the system behaving as a lossy element in the cavity. The contribution to the cavity loss rate is $\kappa_{sc} = 12\pi^2\omega(V^2/\lambda^3 V_c)\left(\frac{\epsilon-1}{\epsilon+2}\right)^2$, where V_c is the cavity mode volume, and is typically much smaller than the natural cavity linewidth κ. We also emphasize that in the Lamb-Dicke regime, the scattering does not cause extra decoherence

beyond that from recoil heating. This is in contrast to motional wavepackets of spatial extent $\Delta x \sim \lambda$, where a single scattering event can destroy quantum coherence [32].

II. COOLING THE CENTER-OF-MASS MOTION TO THE GROUND STATE

We now describe the optical cooling effect of the weaker, second cavity mode (denoted mode 2). For concreteness, we assume that the sphere is trapped near the anti-node $x = 0$ of cavity mode $E_1 \propto \cos\ k_1 x$, and that the second mode has spatial profile $E_2 \propto \cos\,(k_2 x - \pi/4)$, such that the intensity gradient is maximized. The total Hamiltonian of the system is given in a rotating frame by

$$\begin{aligned} H \;=\; & -\hbar\delta_1 \hat{a}_1^\dagger \hat{a}_1 - \hbar\delta_2 \hat{a}_2^\dagger \hat{a}_2 + \frac{\hbar\Omega}{2}\left[(\hat{a}_1 + \hat{a}_1^\dagger) + \sqrt{2\zeta'}(\hat{a}_2 + \hat{a}_2^\dagger)\right] \\ & -\hbar g_1(\cos\ 2k_1\hat{x} - 1)\hat{a}_1^\dagger \hat{a}_1 - \hbar g_2 \cos\ 2(k_2\hat{x} - \pi/4)\hat{a}_2^\dagger \hat{a}_2 + \frac{\hat{p}^2}{2m}. \end{aligned} \tag{4}$$

Here $\hat{p}, \hat{x}$ are the momentum and position operators of the CM, $\hat{a}_i$ is the photon annihilation operator of cavity mode i, and Ω, $\Omega\sqrt{2\zeta'}$ are the driving amplitudes of modes 1 and 2, respectively. δ_i is the detuning between the driving field and mode frequency when the sphere sits at $x = 0$. The opto-mechanical coupling strengths $g_i = \frac{3V}{4V_{c,i}}\frac{\epsilon-1}{\epsilon+2}\omega_i$ characterize the position-dependent frequency shifts due to the sphere (see Appendix), where $V_{c,i}$, ω_i are the mode volume and resonance frequency of mode i. To simplify notation, we assume that modes $1, 2$ have similar properties, $\omega_1 \approx \omega_2 = \omega$, etc. In addition to the evolution described by H, the system also exhibits cavity losses and the mechanical noise described previously.

Expanding the opto-mechanical coupling term of mode 2 around $x = 0$, $\hbar g \cos\ 2(k\hat{x} - \pi/4)\hat{a}_2^\dagger \hat{a}_2 \approx 2\hbar g k \hat{x} \hat{a}_2^\dagger \hat{a}_2$, one finds a linear coupling in the sphere position, analogous to the effect of radiation pressure on a moving mirror of a Fabry-Perot cavity [10]. Physically, the motion induces changes in the detuning and thus the intra-cavity field amplitude, while the lag in the cavity response enables the field to do work (cooling) on the sphere. To calculate the cooling rate, following the techniques of Ref. [10] we first apply shifts to the operators, $\hat{a}_i \to \hat{a}_i + \alpha_i$, $\hat{x} \to \hat{x} + x_0$, where α_i and $x_0 \approx \zeta/k$ ($\zeta \approx \kappa^2\zeta'/(\kappa^2 + 4\delta_2^2)$) are mean values of the quantum fields. Here we have defined $2\zeta = |\alpha_2/\alpha_1|^2$ as the ratio of intra-cavity intensities of modes 1 and 2, and assumed that mode 1 is driven on resonance ($\delta_1 = 0$). To lowest order in ζ, field mode 1(2) is purely responsible for trapping (cooling). Subsequently tracing out the cavity degrees of freedom yields equations for the mechanical motion alone.

In particular, to lowest order in ζ and for $\delta_2 < 0$, the cooling laser provides a net cooling rate $\Gamma \equiv R_{opt,-} - R_{opt,+} = \kappa\Omega_m^2 \left[((\delta_2+\omega_m)^2+(\kappa/2)^2)^{-1} - ((\delta_2-\omega_m)^2+(\kappa/2)^2)^{-1}\right]$ (see Appendix), where $R_{opt,\mp}$ denote the anti-Stokes (cooling) and Stokes (heating) scattering rates (see Fig. 1b). Here $\Omega_m \equiv 2gkx_m|\alpha_1|\sqrt{2\zeta}$ is the effective opto-mechanical driving amplitude (see Fig. 1b) and $x_m \equiv \sqrt{\hbar/2m\omega_m}$. Validity of these perturbative results requires $\Omega_m \lesssim \kappa, \omega_m$ and $\zeta \lesssim 1$.

In the realistic limit that background gas collisions are negligible, the steady-state phonon number is $\langle n_f\rangle \approx \tilde{n}_f + \gamma_{sc}/\Gamma$, where $\tilde{n}_f = R_{opt,+}/\Gamma$ is the fundamental limit of laser cooling [10]. It is minimized when $\delta_2 = -(1/2)\sqrt{\kappa^2+4\omega_m^2}$. In particular, when sideband resolution is achieved ($\omega_m \gtrsim \kappa$), $\tilde{n}_{f,\mathrm{min}} \approx (\kappa/4\omega_m)^2 \ll 1$, indicating that ground-state cooling is possible provided other heating mechanisms are made sufficiently small. Considering the limit $\omega_m \gg \kappa$ and taking the maximum cooling rate $\Gamma \sim \kappa$ consistent with the perturbative calculations, using Eq. (3) one can then re-write $\langle n_f\rangle$ as

$$\langle n_f\rangle \approx \frac{\kappa^2}{16\omega_m^2} + \phi\frac{\omega_m}{\kappa}. \qquad (\omega_m \gg \kappa) \tag{5}$$

The last term on the right corresponds to photon recoil heating and $\phi = (4\pi^2/5)(V/\lambda^3)\frac{\epsilon-1}{\epsilon+2}$ is a dimensionless parameter characterizing the sphere volume. Eq. (5) is minimized for $\kappa/\omega_m = 2\phi^{1/3}$, in which case $\langle n_f\rangle_{\mathrm{min}} = 3\phi^{2/3}/4 \propto (r/\lambda)^2 \ll 1$. Thus, one sees that ground-state cooling is readily attainable (provided that $\zeta \lesssim 1$ can be simultaneously satisfied). Physically, the optimum value of κ/ω_m balances good sideband resolution and excessive heating when large intensities are used to increase ω_m.

To illustrate these results, we consider a sphere of radius $r = 50$ nm and $\omega_m/(2\pi) = 0.5$ MHz levitated inside a cavity of length $L = 1$ cm and mode waist $w = 25$ μm ($V_c = (\pi/4)Lw^2$). In Fig. 2a we plot the minimum obtainable $\langle n_f\rangle$ (black curve) as a function of cavity finesse $\mathcal{F} \equiv \pi c/2\kappa L$, assuming negligible gas collisions and subject to the constraints $\zeta, \Omega_m/\kappa, \Omega_m/\omega_m < 1/2$ and optimized over detuning δ_2. For low cavity finesse the cooling is essentially limited by sideband resolution ($\tilde{n}_{f,\mathrm{min}}$, red curve) and the ground state regime $\langle n_f\rangle \sim 1$ can be reached with a finesse of $\mathcal{F} \sim 3600$. A minimum of $\langle n_f\rangle \sim 0.02$ is reached at a finesse of $\mathcal{F} \sim 50000$ (with corresponding cooling rate $\Gamma \sim 10^6$ s^{-1}). This corresponds to a final temperature of $T_f \sim 6$ μK, or a remarkable compression factor of $T/T_f \sim 5\times10^7$ relative to room temperature T.

III. MOTIONAL ENTANGLEMENT AND SQUEEZED LIGHT GENERATION USING QUANTUM STATE TRANSFER

A number of related schemes have been proposed for quantum state transfer between light and the motion of atoms [12, 13] or nano-mechanical systems [14, 15]. In our system, the small mechanical noise and ease of achieving good sideband resolution in principle allow state transfer to be realized with almost perfect efficiency. This might enable light with non-classical properties to be mapped onto mechanical motion, and as an example, we show that this can be used to generate EPR correlations between two spatially separate spheres. Moreover, a complementary process can be realized, where a non-trivial mechanical state (a squeezed state) is prepared through coherent manipulation and subsequently transferred to light leaving the cavity. The latter case illustrates how opto-mechanics can yield a novel nonlinear optical system.

First we give a simplified picture of quantum state transfer using a one-sided, ideal cavity (where all losses are via transmission through one cavity mirror) [33]. Specifically, we consider the Heisenberg equations of motion in a rotating frame for the cavity cooling mode and the motion (after applying the shifts described in the previous section), when the cooling mode is driven resonantly on the red motional sideband ($\delta_2 = -\omega_m$),

$$\begin{aligned} \frac{d}{dt}\hat{a}_2 &= -\frac{\kappa}{2}\hat{a}_2 - i\Omega_m\left(\hat{b} + \hat{b}^\dagger e^{2i\omega_m t}\right) + \sqrt{\kappa}\hat{a}_{2,\mathrm{in}}, \\ \frac{d}{dt}\hat{b} &= (i/\hbar)[H_e, \hat{b}] - i\Omega_m\left(\hat{a}_2 + \hat{a}_2^\dagger e^{2i\omega_m t}\right) + i\hat{F}(t)e^{i\omega_m t}. \end{aligned} \tag{6}$$

The Hamiltonian H_e describes any external forces or couplings applied to the sphere beyond those in Eq. (4), $\hat{b}$ is the annihilation operator corresponding to a harmonic oscillator of mass m and frequency ω_m, and $\hat{a}_{2,\mathrm{in}}$ is the cavity input operator associated with losses. $F(t)$ is the (Hermitian) noise due to photon recoil, which has correlations $\langle F(t)F(t')\rangle = \phi\omega_m\delta(t-t')$, and we assume all other noise is negligible. Since the cavity trapping mode ($\hat{a}_1$) effectively provides a harmonic potential and can otherwise be ignored, for simplicity we will omit the subscript 2 as we refer to the cooling mode in future discussions. Temporarily assuming that the non-secular terms ($e^{2i\omega_m t}$) can be ignored and that the mechanical motion evolves slowly on time scales compared to $1/\kappa$, one can adiabatically eliminate the cavity mode to yield $\hat{a} \approx -2i(\Omega_m/\kappa)\hat{b} + (2/\sqrt{\kappa})\hat{a}_{\mathrm{in}}$, and $d\hat{b}/dt \approx (i/\hbar)[H_e, \hat{b}] - (\Gamma/2)\hat{b} - i\sqrt{\Gamma}\hat{a}_{in} + i\hat{F}(t)e^{i\omega_m t}$, where $\Gamma \equiv 4\Omega_m^2/\kappa$ is the cavity-induced cooling rate in the weak-driving limit ($\Omega_m \lesssim \kappa$). The cavity

output is related to the input and intra-cavity fields through $\hat{a}_{\rm out} = \sqrt{\kappa}\hat{a} - \hat{a}_{\rm in}$ [33], or $\hat{a}_{\rm out} \approx -i\sqrt{\Gamma}\hat{b} + \hat{a}_{\rm in}$, which states that the mechanical motion is mapped onto the outgoing light. Physically, the cooling process converts phononic excitations into photonic excitations that leak out of the cavity. Generally, two mechanisms will degrade state transfer. First, $\hat{F}$ adds extra noise to the ideal state that one is attempting to transfer, with a strength characterized by the small parameter ϕ. Second, the non-secular terms contribute to Stokes scattering, destroying the perfect phonon-photon correspondence, with a strength that is expected to be proportional to $(\kappa/\omega_m)^2$. Given that $\phi, (\kappa/\omega_m)^2$ can be made small, nearly perfect state transfer is possible in principle. We illustrate this with two examples, entanglement transfer and squeezed light generation.

A. Entanglement transfer

Here we describe how EPR correlations shared between two modes of light [17] can be mapped to the motion of two spheres trapped in spatially separate cavities. Specifically, we define quadrature operators for the input light for each of the two systems (denoted A, B), given by $X^{(j)}_{+,\rm in} = (\hat{a}^{(j)}_{\rm in} + \hat{a}^{(j)\dagger}_{\rm in})$, $X^{(j)}_{-,\rm in} = (\hat{a}^{(j)}_{\rm in} - \hat{a}^{(j)\dagger}_{\rm in})/i$ for $j = A, B$. A similar set of operators $X^{(j)}_{\pm,m}, X^{(j)}_{\pm,\rm out}$ can be defined for the motion and output light, by replacing $\hat{a}^{(j)}_{\rm in} \to \hat{b}^{(j)}, \hat{a}^{(j)}_{\rm out}$, respectively. Of particular interest is the case where the two input fields exhibit broadband EPR correlations between them,

$$\langle (X^{(A)}_{+,\rm in}(\omega) + X^{(B)}_{+,\rm in}(\omega))^2 \rangle/2 = \langle (X^{(A)}_{-,\rm in}(\omega) - X^{(B)}_{-,\rm in}(\omega))^2 \rangle/2 = e^{-2R} < 1. \tag{7}$$

When the variances satisfy $e^{-2R} < 1$, the two modes exhibit correlations below vacuum level and are entangled [34] (for concreteness, we assume the other combinations of quadratures satisfy $\langle (X^{(A)}_{\pm,\rm in}(\omega) \mp X^{(B)}_{\pm,\rm in}(\omega))^2 \rangle/2 = e^{2R}$). Such EPR correlations have been observed with light and in the internal degrees of freedom of atomic ensembles [35], but have yet to be demonstrated using mechanical systems.

To proceed, we solve Eq. (6) in the Fourier domain (including the non-secular terms) for each of the systems for the correlations given in Eq. (7) and $H_e = 0$. Generally, the non-secular terms yield an infinite set of algebraic equations (coupling frequencies $\omega_m + 2n\omega_m$ for integer n), which given $\omega_m \gg \Omega_m, \kappa$ can be truncated to good approximation at $n > 1$. For simplicity of analysis, we assume the two systems have identical properties, and that

the cooling rate $\Gamma \sim \kappa$. However, we expect our results should qualitatively hold provided that only Γ, ω_m of the two systems are properly tuned, which can be easily accomplished by adjusting the trapping and cooling beam intensities. One can then show that state transfer yields the following joint variances in the motion (see Appendix),

$$\Delta_{\mathrm{EPR}} \equiv \langle (X^{(A)}_{\pm,m}(t) \mp X^{(B)}_{\pm,m}(t))^2 \rangle / 2 = e^{-2R} + \frac{\kappa^2}{16\omega_m^2}(3e^{2R} + 2\sinh 2R) + \frac{4\phi\omega_m}{\kappa}. \qquad (8)$$

As expected, Stokes scattering and recoil heating contribute to the variance by amounts $(\kappa/\omega_m)^2$ and $\phi\omega_m/\kappa$, respectively. This can be minimized with respect to κ/ω_m, yielding $\Delta_{\mathrm{EPR,min}} = e^{-2R} + 3(\phi/2)^{2/3}(3e^{2R} + 2\sinh\ 2R)^{1/3}$. To illustrate these results we plot $\Delta_{\mathrm{EPR,min}}$ in Fig. 2b as a function of e^{-2R}, taking the same parameters as in Fig. 2a. For the moderate values of e^{-2R} typically obtained in experiments [17], EPR correlations in the motion can be achieved with reasonable cavity finesse $F < 10^5$.

B. Squeezed light generation

First we describe a technique to create a mechanical squeezed state, and then derive the properties of the outgoing light upon quantum state transfer. Mechanical squeezing is accomplished by adding a sinusoidally-varying component to the intensity of the trapping beam, which yields the Hamiltonian of a parametric amplifier [36], $H_e = \epsilon_m \omega_m^2 x^2 \sin\ 2\omega_m t$. Here ϵ_m is a small parameter characterizing the strength of the modulation of the trap frequency. As one approaches the threshold for parametric oscillation ($\epsilon_m\omega_m \to \Gamma$), the variance in one quadrature of motion is reduced by up to a factor of 2 [36].

We now investigate the properties of the outgoing light over a narrow frequency range near the cavity resonance, specifically considering $X_{\pm,\mathrm{out}}(\omega = 0)$. We apply similar methods as above to solve Eq. (6) in the Fourier domain. Taking the limit as one approaches threshold and $\Gamma \sim \kappa$, the variance in the output light is given by (see Appendix)

$$\Delta X^2_{+,\mathrm{out}}(\omega = 0) = \frac{2\phi\omega_m}{\kappa} + \frac{5}{16}\frac{\kappa^2}{\omega_m^2}. \qquad (9)$$

Again, an optimum value of $\kappa/\omega_m \propto \phi^{1/3}$ maximizes the squeezing, with $(\Delta X^2_{+,\mathrm{out}})_{\mathrm{min}} \approx 2.04\phi^{2/3}$ (note that $\Delta X^2_{+,\mathrm{out}} = 1$ for vacuum). A plot of $(\Delta X^2_{+,\mathrm{out}})_{\mathrm{min}}$ as a function of sphere size is shown in Fig. 2c. For $r = 10$ nm size spheres, one finds that over 25 dB of squeezing relative to vacuum can be obtained using an ideal cavity (note

for good vacuum conditions, background gas collisions are negligible down to $r{\sim}5$ nm). In practice, a cavity has additional scattering and absorption losses that limit the squeezing. Taking an ultra-high finesse cavity with $\sim$1 ppm losses per round trip [37] and a set of reasonable cavity dimensions, we show in the Appendix that light squeezed by up to $\sim$15 dB can be extracted.

In principle, similar techniques also apply to trapped atoms or ions. However, one benefits from the relatively large mass m of the sphere. Specifically, approaching threshold, one quadrature of motion becomes infinitely unsqueezed, producing a large position uncertainty Δx [36]. At the same time, faithful quantum state transfer requires a linear opto-mechanical coupling, which translates into a requirement that the Lamb-Dicke parameter $\eta{\equiv}k\Delta x \propto m^{-1/2}{\ll}1$ be small. In the Appendix, we show that $\eta{\ll}10^{-2}$ can be satisfied with a sphere even in the regime of $\sim$25 dB squeezing levels. To compare, a typical atom trapped with a frequency of $\omega_m/(2\pi){\sim}1$ MHz in its *ground state* already yields $\eta{\sim}0.05$.

IV. OUTLOOK

An optically levitated opto-mechanical system can have remarkably long coherence times, which potentially enables quantum phenomena such as entanglement to be observed even in room-temperature environments. Combining previously demonstrated techniques to controllably grow small particles [38] and load and manipulate them in vacuum [6, 39] should put this system within experimental reach. Extending the ideas presented here should open up several other interesting possibilities. For example, beyond the dipole-type objects considered here, one could engineer the shapes of the levitated objects to yield even larger mechanical frequencies and coherence times, and controllably study the decoherence of a large system [40]. Also, several spheres or more complex nano-mechanical systems with internal modes could be levitated and coupled together, for the purpose of entangling multiple degrees of freedom. Separately, one could take advantage of the fact that the potential for the CM is purely optical to engineer non-trivial dynamics, such as nonlinear motion. It would also be interesting to develop analogous levitation techniques using nano- and micro-photonic cavities [41, 42], combining their remarkable optical properties with the excellent mechanical characteristics of a trapped particle. Finally, by levitating charged or magnetic systems, one could potentially realize systems analogous to ion traps [43] or facilitate novel

quantum hybrid architectures [44].

Acknowledgments

DC and SP acknowledge support from the Gordon and Betty Moore Foundation through Caltech's Center for the Physics of Information, DC from the National Science Foundation under Grant No. PHY-0803371, CR from a Millikan Postdoctoral Fellowship, and JY and PZ from a Moore Fellowship during their stay at Caltech. Work at Innsbruck is supported by the Austrian Science Fund and EU Projects.

Note added: We also have become aware of a recent, similar proposal to optically levitate and manipulate a nano-mechanical system by O. Romero-Isart *et al.*, in arXiv:0909.1469 (2009).

APPENDIX A: ELECTRODYNAMIC CALCULATION OF FORCES ON DIELECTRIC SPHERE

Here we describe in detail the point-dipole approximation for a sub-wavelength dielectric sphere, and compare the results of this approximation with exact numerical electrodynamic calculations of the optical forces. For concreteness, we consider a dielectric sphere of (possibly complex) permittivity ϵ and radius r, interacting with an incident standing electromagnetic wave with electric and magnetic field components $\mathbf{E}_{\rm in} = \hat{x}E_0 \cos\, k(z-z_0)\cos\,\omega t$ and $\mathbf{B}_{\rm in} = \hat{y}(E_0/c)\sin\, k(z-z_0)\sin\,\omega t$ ($k = \omega/c$). Here we assume that the sphere is in free space rather than in a cavity, which allows one to unambiguously calculate the optical forces acting on the sphere independent of its motion (as opposed to the cavity case where the motion of the sphere generally shifts the cavity resonance, causing the intra-cavity field $E_0(t)$ to depend on the history of motion). In the special case where the sphere is localized near one of the nodes or anti-nodes, the free-space and cavity cases yield the same results (*e.g.*, for the mechanical trap frequency ω_m) as the cavity resonance and intra-cavity field to lowest order become insensitive to small displacements of the sphere. The electrodynamic problem of plane-wave scattering off of a sphere is exactly solvable, as the vector wave equation $\nabla^2\mathbf{E}(\mathbf{r}) + k^2\epsilon(\mathbf{r})\mathbf{E}(\mathbf{r}) = 0$ (with similar equation for $\mathbf{B}$) admits solutions through separation of variables [45]. Note that one can define natural length scales $k|\sqrt{\epsilon}|r$, kr for

the electrodynamic response inside and outside the sphere. Of particular interest is the case when $k|\sqrt{\epsilon}|r \ll 1$ is a small parameter (we assume that $|\sqrt{\epsilon}| > 1$ for this discussion, which is typically the case). One can then formally solve the wave equations using perturbation theory, with the lowest order equation given by $\nabla^2 \mathbf{E}(\mathbf{r}) = 0$ along with appropriate boundary conditions at the surface of the sphere. Physically, this approximation states that the magnetic field is not important in the near-field, such that the lowest-order response of the sphere can be obtained by solving an electrostatic equation. Taking an optical wavelength of $\lambda = 2\pi/k = 1$ μm and $\epsilon = 2$, for instance, the electrostatic solution should be valid for $r \lesssim 110$ nm. In this regime, the polarizablity of the sphere is of the simple form given by electrostatic theory, $\alpha_{\text{ind}} = 3\epsilon_0 V \frac{\epsilon-1}{\epsilon+2}$ [45], as is used in the main text. The optical potential experienced by the sphere is predicted to be $U_{\text{opt}} = -(1/4)(\text{Re}\,\alpha_{\text{ind}})E_0^2 \cos^2 k(z - z_0)$. For spheres larger than $r \gtrsim 1/k|\sqrt{\epsilon}|$, the forces predicted by the electrostatic theory will be substantially larger than the actual forces, as phase variations of the field within the sphere become important.

To compare the electrostatic approximation with actual results, we first solve the electrodynamic scattering problem exactly. The exact force F_z along z can then be obtained by integrating the Maxwell stress tensor T_{ij} over the sphere surface S,

$$F_z = \epsilon_0 \oint_S da \sum_{j=x,y,z} T_{zj} \hat{n}_j, \tag{A1}$$

where $\hat{n}_j$ is the outgoing normal vector to the sphere surface. In Fig. 3 we compare the approximate and exact forces for various values of r, taking $\epsilon = 2$. It can be seen that the two methods agree closely for $k\sqrt{\epsilon}r \lesssim 1$. For spheres where $k\sqrt{\epsilon}r \gtrsim 1$, the forces predicted from electrostatic theory can be much larger than the actual forces, and even different in sign.

APPENDIX B: ABSORPTION LOSSES OF TRAPPED SPHERE

In this section, we consider the effect that a small imaginary component of the permittivity ϵ has on a trapped sphere. In the limit that the sphere has a radius much smaller than the optical wavelength, the sphere behaves as a point-like dipole with polarizability $\alpha_{\text{ind}} = 3\epsilon_0 V \left(\frac{\epsilon-1}{\epsilon+2}\right)$. For small Im ϵ, the polarizability acquires a small imaginary component

that leads to a non-zero absorption cross-section, with a corresponding absorbed power

$$P_{\rm abs} = 12\pi \frac{I_0}{\lambda} V \mathrm{Im}\, \frac{\epsilon - 1}{\epsilon + 2}. \tag{B1}$$

Here I_0 is the trapping beam intensity, V is the sphere volume, and λ is the optical wavelength. The absorbed power causes a rise in the internal temperature $T_{\rm int}$ of the sphere, which is balanced out by thermalization with a background gas and blackbody radiation.

We first quantify the effect of the background gas (which is negligible in the regime of particular interest where the sphere is trapped under good vacuum conditions). There are two limiting regimes to the background gas interactions, where the sphere radius is either much smaller or larger than the molecular mean free path $\lambda_{\rm mfp}$. At a relatively large pressure of $P = 1$ Torr and room temperature, $\lambda_{\rm mfp} \sim 100$ μm and thus our case of interest is always $r \ll \lambda_{\rm mfp}$. Here, gas molecules independently collide and partially thermalize with the sphere. This leads to a cooling rate [46]

$$\frac{dE}{dt} = -\alpha_g \sqrt{\frac{2}{3\pi}} (\pi r^2) P v_{\rm rms} \frac{\gamma_{\rm sh} + 1}{\gamma_{\rm sh} - 1} \left(\frac{T_{\rm int}}{T} - 1 \right), \tag{B2}$$

where $P, v_{\rm rms}, T$ are the background gas pressure, root-mean-square speed, and temperature, respectively, and $\gamma_{\rm sh}$ is the gas specific heat ratio ($\gamma_{\rm sh} = 7/5$ for an ideal diatomic gas). α_g is a phenomenological energy accommodation factor ($0 \leq \alpha_g \leq 1$), which characterizes the degree to which a gas molecule thermalizes with the sphere upon a single collision.

Under good vacuum conditions, blackbody radiation dissipates the majority of the power absorbed by the sphere. For the sub-micron spheres we are considering, the radius is much smaller than the absorption length at typical blackbody radiation wavelengths, and thus the usual formulas for blackbody radiated power do not apply. Instead, the sphere again behaves as a point-like dipole at these wavelengths, *e.g.*, the radiated power scales like volume (as opposed to surface area in the case of a large object). The internal heating rate due to blackbody radiation is given by $dE/dt = \sum_{\mathbf{k}} (\hbar c k) R_{{\rm abs},\mathbf{k}}$, where the sum is over all blackbody radiation modes (and polarizations), $\mathbf{k}$ is the wavevector of each mode, and $R_{{\rm abs},\mathbf{k}}$ is the absorption rate of each mode. It is given by

$$R_{{\rm abs},\mathbf{k}} = 3ck(V/V_q) n_k \mathrm{Im} \left(\frac{\epsilon(\omega_k) - 1}{\epsilon(\omega_k) + 2} \right), \tag{B3}$$

where $n_k = (e^{\hbar c k / k_B T} - 1)^{-1}$ is the occupation number of each mode and V_q is the quantization volume. Assuming that the sphere has a relatively constant and temperature-independent

permittivity $\epsilon(\omega)\approx\epsilon_{\rm bb}$ across the blackbody radiation spectrum, it is straightforward to show that the sphere absorbs blackbody radiation at a rate

$$\frac{dE}{dt} = \frac{72\zeta(5)}{\pi^2}\frac{V}{c^3\hbar^4}\mathrm{Im}\left(\frac{\epsilon_{\rm bb}-1}{\epsilon_{\rm bb}+2}\right)(k_B T)^5, \tag{B4}$$

where T is the background temperature and $\zeta(5)\approx 1.04$ is the Riemann zeta function. Similarly, the sphere radiates blackbody energy at a rate given by the negative of Eq. (B4), with the substitution $T\to T_{\rm int}$.

To illustrate these results, in Figs. 4a-c we plot the internal equilibrium temperature $T_{\rm int}$ of the sphere as a function of background gas pressure and trapping intensity I_0. Here we have taken into account the effects of optical absorption (Im ϵ), thermalization with the background gas, and blackbody radiation. The values of Im ϵ in Figs. 4a,b,c correspond to bulk optical absorption rates of $10, 100, 1000$ dB/km, respectively, while the real part of the permittivity is chosen to be Re $\epsilon = 2$. We have taken the other parameters to be $r = 50$ nm, $\alpha_g = 0.25$, Im $\frac{\epsilon_{\rm bb}-1}{\epsilon_{\rm bb}+2} = 0.1$ (roughly corresponding to the averaged value of fused silica around blackbody wavelengths [47]), and a volumetric heat capacity of the sphere of $\tilde{c} = 2$ J/m^3·K. Note that at sufficiently low pressures, the temperature becomes pressure-independent as only blackbody radiation significantly contributes to energy dissipation (as indicated by the vertical contours in the figure). Furthermore, in this regime the final temperature is independent of the sphere size (provided that $r\ll\lambda$), since both the optical absorption and blackbody radiation scale linearly with volume. For losses of $\sim$10 dB/km, one finds that over 10 W/μm^2 of power can be sustained without exceeding the melting point of a typical material.

APPENDIX C: DERIVATION OF OPTO-MECHANICAL COUPLING STRENGTH

Generally, introducing a dielectric material into an optical cavity causes the bare resonant frequency ω of a cavity mode to shift by an amount $\delta\omega$, which in perturbation theory is given by [48]

$$\frac{\delta\omega}{\omega} = -\frac{1}{2}\frac{\int d^3\mathbf{r}\ \delta P(\mathbf{r})\cdot\mathbf{E}(\mathbf{r})}{\int d^3\mathbf{r}\ \epsilon_0\mathbf{E}^2(\mathbf{r})}. \tag{C1}$$

Here $\mathbf{E}(\mathbf{r})$ is the bare cavity mode profile and $\delta P(\mathbf{r})$ is the variation in permittivity introduced by the dielectric object. Considering the case where the dielectric object is a sub-wavelength

sphere, its dielectric response is well-approximated by a point dipole, $P(\mathbf{r}')\approx\alpha_{\rm ind}E(\mathbf{r})\delta(\mathbf{r}-\mathbf{r}')$, where $\mathbf{r}$ is the center-of-mass (CM) position of the sphere. Taking a mode profile $E\propto\cos(kx-\phi)$, one readily finds (up to a constant shift) that

$$\delta\omega = -\frac{3V}{4V_c}\frac{\epsilon-1}{\epsilon+2}\cos(2kx-2\phi)\omega. \tag{C2}$$

The interaction Hamiltonian between this optical mode and the mechanical motion is subsequently given by $H_{\rm om}=\hbar\delta\omega\hat{a}^\dagger\hat{a}$, and as in the main text, one can define a characteristic opto-mechanical coupling strength $g=\frac{3V}{4V_c}\frac{\epsilon-1}{\epsilon+2}\omega$.

APPENDIX D: OPTICAL SELF-COOLING EQUATIONS

Here we derive in detail the cooling rate equations for the CM motion of the sphere, whose results are summarized in the main text. We begin with the Hamiltonian given by Eq. (4) in the main text. The corresponding Heisenberg equations of motion, including dissipation, are

$$\begin{aligned}
\frac{d}{dt}\hat{a}_1 &= (i\delta_1-\kappa/2)\hat{a}_1 - \frac{i\Omega}{2} + \sqrt{\kappa}\hat{a}_{1,\rm in},\\
\frac{d}{dt}\hat{a}_2 &= (i(\delta_2+2gk\hat{z})-\kappa/2)\hat{a}_2 - \frac{i\Omega}{2}\sqrt{2\zeta'} + \sqrt{\kappa}\hat{a}_{2,\rm in},\\
\frac{d}{dt}\hat{p} &= -4\hbar gk^2\hat{a}_1^\dagger\hat{a}_1\hat{z} + 2\hbar gk\hat{a}_2^\dagger\hat{a}_2 - \gamma\hat{p}/2 + \hat{F}_p(t),\\
\frac{d}{dt}\hat{x} &= \frac{\hat{p}}{m}.
\end{aligned} \tag{D1}$$

Here $\hat{a}_{i,\rm in}$ are input-field operators associated with the cavity mode losses κ, γ is the damping rate of the motion, and $\hat{F}_p$ is the noise force acting on the sphere. In the above equations, we have expanded the position-dependent opto-mechanical coupling terms $g_i\cos 2(k_i\hat{x}-\phi_i)$ to first order in the displacement $\hat{x}$, and for simplicity have assumed that the two cavity modes have similar properties ($g_1\approx g_2=g$, etc.). We now apply shifts to all of the operators, $\hat{a}_i\to\hat{a}_i+\alpha_i$, $\hat{x}\to\hat{x}+x_0$, where the constants x_0 and α_i are chosen to cancel out all of the constant terms in the equations of motion. This yields

$$\alpha_1 = -\frac{i\Omega}{\kappa}, \tag{D2}$$

$$\alpha_2 = -\frac{i\Omega}{2}\frac{\sqrt{2\zeta'}}{(\kappa/2)-i\delta_2'}, \tag{D3}$$

where $\delta_2' = \delta_2 + 2gkx_0$ is the detuning relative to the new resonance frequency of the cavity when the sphere sits at $x = x_0$ rather than $x = 0$. Physically, $x = x_0$ corresponds to the minimum of the total optical potential formed by the two driven cavity modes. We define the ratio of the cavity mode intensities to be $2\zeta \equiv |\alpha_2/\alpha_1|^2$, which is equivalent to $\zeta = \zeta'\kappa^2/(\kappa^2 + 4\delta_2'^2)$. In terms of ζ, the shifted equilibrium position is given by $kx_0 = \zeta$. Clearly then the expansion in $\hat{x}$ of the opto-mechanical coupling terms requires that ζ be small. For simplicity, the prime symbol in δ_2' will be implicitly understood, and we also take $\delta_1 = 0$ in the following discussions. Following the shifts to the operators $\hat{a}_i$ and $\hat{x}$ and then linearizing the equations of motion, one finds

$$\begin{aligned}
\frac{d}{dt}\hat{a}_1 &= -4igk^2x_0\alpha_1\hat{x} - (\kappa/2)\hat{a}_1 + \sqrt{\kappa}\hat{a}_{1,\mathrm{in}}, \\
\frac{d}{dt}\hat{a}_2 &= (i\delta_2 - \kappa/2)\hat{a}_2 + 2ig\alpha_2 k\hat{x} + \sqrt{\kappa}\hat{a}_{2,\mathrm{in}}, \\
\frac{d}{dt}\hat{p} &= -4\hbar gk^2|\alpha_1|^2\hat{x} + 2\hbar gk\left(\alpha_2\hat{a}_2^\dagger + \alpha_2^*\hat{a}_2 - 2kx_0(\alpha_1\hat{a}_1^\dagger + \alpha_1^*\hat{a}_1)\right) - \gamma\hat{p}/2 + \hat{F}_p(t), \\
\frac{d}{dt}\hat{x} &= \hat{p}/m.
\end{aligned} \tag{D4}$$

Note that cavity mode 1 provides a linear restoring force $d\hat{p}/dt \sim -4\hbar gk^2|\alpha_1|^2\hat{x} = -m\omega_m^2\hat{x}$, and it is straightforward to show that this relation leads to the expression for the harmonic oscillator frequency ω_m given in Eq. (1) of the main text. Furthermore, note that the sphere is opto-mechanically coupled to mode 1 with an amplitude $4gk^2x_0\alpha_1 \propto \zeta$, and to mode 2 with an amplitude $2gk\alpha_2 \propto \sqrt{\zeta}$. Thus, to lowest order in ζ, modes 1 and 2 are purely responsible for optical trapping and cooling, respectively. Treating mode 1 simply as an external harmonic potential for the sphere, the opto-mechanical system comprised of the CM motion of the sphere and cavity mode 2 is completely equivalent to the system described in Ref. [10]. In particular, the optical self-heating and self-cooling rates $R_\pm$ given in the main text follow immediately. For convenience, we also re-define the phases of the operators to make the opto-mechanical driving amplitude $\Omega_m = 2\hbar gk\alpha_2 = 2\hbar gk\alpha_1\sqrt{2\zeta}$ real.

APPENDIX E: NOISE FORCES ACTING ON TRAPPED SPHERE

In the main text, we have derived the motional heating rates of the sphere due to background gas collisions and photon recoil kicks, which under realistic conditions are the dominant heating mechanisms. Here, we derive the heating rates for a number of other less

important processes.

1. Photon shot noise

Photon shot noise inside the cavity leads to heating via fluctuations in the mechanical oscillator frequency ω_m. We write the varying mechanical frequency in the form

$$\omega_m^2(t) = \omega_{m,0}^2 \left(1 + \frac{\delta N(t)}{N_0}\right), \tag{E1}$$

where $\omega_{m,0}, N_0$ are the mean frequency and mean photon number in the trapping mode of the cavity, and δN is the number fluctuation of this mode. Following the techniques of Ref. [49], the shot noise leads to parametric transitions (where the phonon number $n \to n \pm 2$ jumps in pairs) at a rate R proportional to the power spectral density of the fluctuations at frequency $2\omega_{m,0}$,

$$R_{n\to n+2} = \frac{\pi\omega_{m,0}^2}{16} S(2\omega_{m,0})(n+2)(n+1), \tag{E2}$$

$$R_{n\to n-2} = \frac{\pi\omega_{m,0}^2}{16} S(2\omega_{m,0}) n(n-1). \tag{E3}$$

Here the power spectral density is defined by

$$S(\omega) = \frac{2}{\pi N_0^2} \int_0^\infty dt \, \cos\, \omega t \, \langle \delta N(t) \delta N(0) \rangle, \tag{E4}$$

which is evaluated to be $S(\omega) = \frac{1}{\pi N_0} \frac{4\kappa}{\kappa^2 + 4\omega^2}$ for a cavity of linewidth κ driven on resonance. Assuming that the sphere initially is in the ground state, the number of oscillations before a quantum jump due to shot noise is

$$N_{\rm osc}^{\rm (sn)} = \frac{\omega_{m,0}}{2\pi R_{0\to 2}} = \frac{\epsilon + 2}{\epsilon - 1} \frac{V_c \rho}{3\pi c \hbar k^3} \frac{\omega_{m,0}}{\kappa} (\kappa^2 + 16\omega_{m,0}^2). \tag{E5}$$

Here, $k = 2\pi/\lambda$ is the wavevector of the trapping beam and V_c is the cavity mode volume. As an example, we consider a cavity of length $L = 1$ cm and waist $w = 25$ μm ($V_c = (\pi/4) L w^2$), a high-index dielectric sphere ($\frac{\epsilon-1}{\epsilon+2} \sim 1$), density $\rho = 2$ g/cm^3, $\lambda = 1$ μm, and trapping frequency $\omega_m/(2\pi) = 0.5$ MHz. $N_{\rm osc}^{\rm (sn)}$ as a function of cavity finesse F ($F = \pi c/2\kappa L$) is plotted in Fig. 5. It can be seen that the number of allowed oscillations is at least of order $N_{\rm osc}^{\rm (sn)} \sim 10^{10}$, which is much larger than the limit due to photon recoil. Physically, the low heating rates are attributable to the large intra-cavity intensities used to achieve $\sim$MHz mechanical oscillation frequencies, which suppresses the fractional noise $\delta N/N_0 \propto N_0^{-1/2}$.

2. Blackbody radiation

As in the case of scattering of laser light, the absorption and emission of blackbody radiation by the sphere also lead to recoil heating. The absorption rate of blackbody radiation of mode $\mathbf{k}$ is given in Eq. (B3) (with each absorption event providing a momentum kick $\hbar k_x$ along the trapping axis), and again we assume that $\epsilon(\omega)\approx\epsilon_{bb}$ is approximately flat across the blackbody radiation spectrum. Summing over all modes, the characteristic jump rate due to absorption of blackbody radiation is then given by (cf. Eq. (2) in main text)

$$\gamma_{\rm bb} = \frac{2\pi^4}{63}\frac{(k_B T)^6}{c^5\hbar^5\rho\omega_m}{\rm Im}\frac{\epsilon_{\rm bb}-1}{\epsilon_{\rm bb}+2}. \tag{E6}$$

The jump rate between harmonic oscillator levels is $R_{n\to n\pm1} = \gamma_{\rm bb}(n+1/2\pm1/2)$. An analogous expression holds for heating via the emission of blackbody radiation, with the replacement $T\to T_{\rm int}$. Note that γ_{bb} is size-independent for small spheres, as both the absorption rate and mass scale linearly with V. Taking as an example a system with $\omega_m/(2\pi)\sim1$ MHz, $\rho = 2$ g/cm^3, Im $\frac{\epsilon_{\rm bb}-1}{\epsilon_{\rm bb}+2} = 0.1$, and $T\sim T_{\rm int}\sim300$ K, we find that the number of oscillations before a quantum jump (due to either absorption or emission) is $N_{\rm osc}^{\rm (bb)}\sim10^{11}$.

3. Anisotropy of sphere

The general problem of the rotational motion of an arbitrary dielectric object inside an optical cavity is quite challenging to solve. Generally, the polarizability $\alpha_{\rm ind}$ becomes a function of its orientation, and changes in its orientation lead to changes in the optical trapping potential and the intra-cavity intensity. Here we consider a simplified version of the problem, where the rotational motion is limited to one axis, and the anisotropy or deformation of the sphere is of spheroid-type. As in the case of the sphere, the latter assumption admits analytical solutions for the polarizability tensor of the object [50]. In particular, we assume that the dielectric is a prolate nanospheroid whose size is much smaller than the optical wavelength, with semi-major axis a and semi-minor axis b, and that the ratio $a/b\approx1$ (*i.e.*, the deviation from an ideal sphere is small). Then the polarizability of the spheroid is given by

$$\alpha_{\rm ind}\approx\alpha_{\rm ind,0}\left(1\pm\frac{9}{20}\frac{\epsilon-1}{\epsilon+2}\left[(a/b)^{4/3}-1\right]\right) \tag{E7}$$

with $\alpha_{\mathrm{ind},0}{\approx}3\epsilon_0 V\frac{\epsilon-1}{\epsilon+2}$. Here the $\pm$ symbols denote when the major and minor axes are aligned along the field polarization axis, respectively. From Eqs. (C1) and (E7), it is straightforward to find the shift in the cavity frequency taking into account the rotational degree of freedom,

$$\delta\omega = \delta\omega_0 + \delta\omega_\theta \cos\, 2\theta, \tag{E8}$$

where $\delta\omega_0$ is the shift associated with the CM position alone (as given by Eq. (C2)), and

$$\delta\omega_\theta = \frac{27}{80}\frac{V}{V_c}\left(\frac{\epsilon-1}{\epsilon+2}\right)^2 \left[(a/b)^{4/3}-1\right]\omega\cos(2kx-2\phi). \tag{E9}$$

Here we have defined θ as the angle of rotation of the spheroid.

We are now interested in deriving the effect of the rotational motion on the CM motion. In analogy with Eq. (D1), the coupled equations of motion between the rotation and the trapping mode are

$$\begin{aligned}
\frac{da_1}{dt} &= -\left(i\delta\omega_\theta\cos\,2\theta+\frac{\kappa}{2}\right)a_1+\frac{i\Omega}{2},\\
\frac{dp_\theta}{dt} &= 2\hbar\delta\omega_\theta|a_1|^2\sin\,2\theta-\gamma_\theta p_\theta+F_\theta(t),\\
\frac{d\theta}{dt} &= \frac{p_\theta}{I_\theta},
\end{aligned} \tag{E10}$$

where p_θ is the angular momentum associated with θ, I_θ is the moment of inertia, and γ_θ, F_θ are the damping coefficient and noise force acting on the rotational motion. Since the rotational energy is of order $\sim k_B T$, it suffices to consider the classical equations given here. The damping term is effected through the background gas, as each collision between the spheroid and a gas molecule partly exchanges angular momentum between the two systems. The damping coefficient is found to be $\gamma_\theta = 5\sqrt{3/(2\pi)}\alpha_\theta P/(v_{\mathrm{rms}} r\rho)$ [51], where $r{\approx}a{\approx}b$. α_θ is a phenomenological accommodation coefficient describing the efficiency of angular momentum transfer. The noise force has correlations $\langle F(t)F(t')\rangle = 2D\delta(t-t')$, where $D=\gamma_\theta k_B T/I_\theta$. Note that γ_θ is a very small quantity under good vacuum conditions.

The full nonlinear coupled equations of Eq. (E10) are difficult to treat in a general setting. However, given the typical smallness of the parameters $\delta\omega_\theta/\kappa$ and $\hbar\delta\omega_\theta|a_1|^2/(k_B T)$ for nearly spherical particles, to lowest order we can ignore the optical coupling to the rotational motion, and the dominant effect of the sphere anisotropy is trap heating through fluctuations in the polarizability α_{ind} rather than intra-cavity intensity fluctuations. This leads to fluctuations in the trap frequency given by

$$\delta\omega_m(t) = \epsilon_\theta\omega_{m,0}\cos\,2\theta(t), \tag{E11}$$

where $\epsilon_\theta = \frac{9}{40}\frac{\epsilon-1}{\epsilon+2}((a/b)^{4/3}-1)$. In analogy with the discussion in Sec. E 1, these fluctuations lead to parametric heating, with a jump rate out of the ground state given by

$$R_{0\to 2} = \int_0^\infty dt\, \cos\, 2\omega_{m,0} t\, \langle \delta\omega_m(0)\delta\omega_m(t)\rangle. \tag{E12}$$

Denoting $\delta\theta(t) = \theta(t) - \theta(0)$, the above equation can be re-written in the form

$$R_{0\to 2} = \frac{1}{2}\int_0^\infty dt\, \cos\, 2\omega_{m,0} t\, (\epsilon_\theta \omega_{m,0}^2)^2 \langle \cos\, 2\delta\theta(t)\rangle. \tag{E13}$$

Making a Gaussian approximation $\langle e^{2i\delta\theta(t)}\rangle \approx \exp(-\langle\delta\theta^2(t)\rangle/2)$, and taking the limit of small γ_θ, one finally finds

$$\frac{R_{0\to 2}}{\omega_{m,0}} = \epsilon_\theta^2 \frac{\sqrt{2\pi}\omega_{m,0}}{8\sqrt{\langle\omega_r^2\rangle}} \exp\left(-\frac{\omega_{m,0}^2}{2\langle\omega_r^2\rangle}\right). \tag{E14}$$

Here $\omega_r = d\theta/dt$ is the angular velocity of the spheroid (typical values of $\sqrt{\langle\omega_r^2\rangle}$ are in the MHz range for sub-wavelength particles). Note that the above function is peaked at $\omega_{m,0} = \sqrt{\langle\omega_r^2\rangle}$, *i.e.*, the parametric heating is most pronounced when the rotational frequency is comparable to the CM oscillation frequency. At this maximum, $R_{0\to 2}/\omega_{m,0} \sim 0.2\epsilon_\theta^2$. Furthermore, for this worst-case scenario, $R_{0\to 2}/\omega_{m,0}$ can be suppressed to the $\sim 10^{-5}$ level with an anisotropy of $a/b \sim 1.03$.

APPENDIX F: ANALYSIS OF ENTANGLEMENT TRANSFER

Here we provide a detailed analysis of entanglement transfer between two modes of light and two spatially separate spheres, leading to Eq. (8) in the main text. The EPR correlations between the two light modes given by Eq. (7) in the main text,

$$\langle (X^{(A)}_{+,\mathrm{in}}(\omega) + X^{(B)}_{+,\mathrm{in}}(\omega))^2\rangle/2 = \langle (X^{(A)}_{-,\mathrm{in}}(\omega) - X^{(B)}_{-,\mathrm{in}}(\omega))^2\rangle/2 = e^{-2R} < 1, \tag{F1}$$

are of the form created by a non-degenerate optical parametic amplifier (NOPA) [52], which we describe below.

The Hamiltonian corresponding to a NOPA with cavity modes A, B is given by

$$H = i\hbar(\beta/2)(\hat{c}^{(A)}\hat{c}^{(B)} - \hat{c}^{(A)\dagger}\hat{c}^{(B)\dagger}), \tag{F2}$$

where $\hat{c}^{(j)}$ is the annihilation operator of mode j. Taking an ideal, one-sided cavity [33], and assuming that the modes have identical linewidths κ_c, the Heisenberg equations of motion for each mode read

$$\frac{d}{dt}\hat{c}^{(j)} = -\frac{\kappa_c}{2}\hat{c}^{(j)} - \frac{\beta}{2}\hat{c}^{(j')\dagger} + \sqrt{\kappa_c}\hat{c}^{(j)}_{\mathrm{in}}. \tag{F3}$$

Here $\hat{c}_{\rm in}^{(j)}$ is the cavity input field for mode j, and $j' = A, B$ for $j = B, A$. The output field is related to the intra-cavity and input fields by $\hat{c}_{\rm out}^{(j)} = \sqrt{\kappa_c}\hat{c}^{(j)} - \hat{c}_{\rm in}^{(j)}$. Writing $\hat{c}^{(j)}(t) = (1/\sqrt{2\pi}) \int d\omega\, e^{-i\omega t}\hat{c}^{(j)}(\omega)$, Eq. (F3) can be exactly solved in the Fourier domain for $\hat{c}^{(j)}(\omega)$. Specifically, defining quadrature operators $\hat{X}_+^{(j)} = \hat{c}^{(j)} + \hat{c}^{(j)\dagger}$ and $\hat{X}_-^{(j)} = (\hat{c}^{(j)} - \hat{c}^{(j)\dagger})/i$ (with analogous definitions for the quadrature operators of the input and output fields), one can show that

$$\hat{X}_{\pm,\rm out}^{(A)}(\omega) \pm \hat{X}_{\pm,\rm out}^{(B)}(\omega) = \frac{\kappa_c - \beta + 2i\omega}{\kappa_c + \beta - 2i\omega} \left(\hat{X}_{\pm,\rm in}^{(A)}(\omega) \pm \hat{X}_{\pm,\rm in}^{(B)}(\omega) \right). \quad (\beta < \kappa_c) \tag{F4}$$

Over a bandwidth $\Delta\omega \ll \kappa_c$ that is much smaller than the cavity linewidth, one can ignore the ω dependence in the equation above, yielding

$$\hat{X}_{\pm,\rm out}^{(A)}(\omega) \pm \hat{X}_{\pm,\rm out}^{(B)}(\omega) = e^{-R} \left(\hat{X}_{\pm,\rm in}^{(A)}(\omega) \pm \hat{X}_{\pm,\rm in}^{(B)}(\omega) \right), \tag{F5}$$

where $e^{-R} = \frac{\kappa_c - \beta}{\kappa_c + \beta}$ for $\beta < \kappa_c$. Physically, for non-zero β, the joint variance of these quadratures in the output fields can display reduced fluctuations relative to the input fields. It can also be shown that the other combinations of the quadratures (for $\Delta\omega \ll \kappa_c$) satisfy

$$\hat{X}_{\pm,\rm out}^{(A)}(\omega) \mp \hat{X}_{\pm,\rm out}^{(B)}(\omega) = e^{R} \left(\hat{X}_{\pm,\rm in}^{(A)}(\omega) \mp \hat{X}_{\pm,\rm in}^{(B)}(\omega) \right), \tag{F6}$$

such that their joint variances become enhanced. For this discussion, the input fields to the NOPA are assumed to be vacuum states.

We now consider the quantum state transfer process for two spheres trapped in spatially separate cavities, where the two output fields generated by NOPA are fed as input fields into each of the opto-mechanical systems. The equations of motion for the two opto-mechanical systems (denoted A, B) are given by Eq. (6) in the main text, with the replacement $\hat{a}_{2,\rm in}^{(j)} = \hat{c}_{\rm out}^{(j)}$. As in the main text, for simplicity we suppress the subscript "2" in the field operators denoting the trapping mode, since we are only interested in this mode from this point on. To solve these equations, we again work in the Fourier domain. Without the fast-rotating terms $e^{2i\omega_m t}$, one could achieve ideal state transfer between the mechanical motion and light, as discussed in the main text. When the fast-rotating terms $e^{2i\omega_m t}$ are included in the analysis, the frequency components $\omega, \omega + 2n\omega_m$ (integer n) of the operators are coupled together in an infinite set of algebraic equations. To make the problem tractable, we truncate this infinite set by ignoring the components $\hat{a}^{(j)}(\omega + 2n\omega_m), \hat{b}^{(j)}(\omega + 2n\omega_m)$ where $|n| \geq 2$ (*e.g.*, we assume $\hat{a}^{(j)}(\omega \pm 4\omega_m) = 0$). This truncation essentially amounts to the assumption that

ω_m is large compared to the other frequency scales in the problem. We then solve the coupled set of equations for $\hat{a}^{(j)}(\omega), \hat{b}^{(j)}(\omega)$ in terms of $\hat{F}^{(j)}(\omega)$ and $\hat{a}^{(j)}_{\rm in}(\omega)$ (or $\hat{c}^{(j)}_{\rm in}(\omega)$), which allows us to obtain any correlation functions for the cavity field or mechanical motion in terms of those of the noise and input fields. The noise forces $\hat{F}^{(j)}$ are assumed to be dominated by photon recoil heating and are independent for the systems A, B, such that their correlations take the form $\langle \hat{F}^{(j)}(\omega) \rangle = 0$ and $\langle \hat{F}^{(j)}(\omega) \hat{F}^{(j')}(\omega') \rangle = \phi \omega_m \delta(\omega + \omega') \delta_{jj'}$, where $\phi = (4\pi^2/5)(V/\lambda^3)\frac{\epsilon - 1}{\epsilon + 2}$ (see main text). We are specifically interested in the quantity

$$\Delta_{\rm EPR} \equiv \langle (X^{(A)}_{\pm,m}(t) \mp X^{(B)}_{\pm,m}(t))^2 \rangle / 2 \tag{F7}$$

characterizing the joint variance in the motion of the two spheres. The solution is generally quite complicated, but can be expanded to lowest order in the small parameter κ/ω_m (it is reasonably assumed that sideband resolution can be achieved, so that $\kappa/\omega_m \ll 1$). After performing this procedure, and also ignoring any fast-rotating terms ($e^{\pm 2i\omega_m t}$) in the final expression for $\Delta_{\rm EPR}$, one arrives at the solution given by Eq. (8) in the main text.

APPENDIX G: ANALYSIS OF SQUEEZED LIGHT GENERATION

Here we derive the squeezing amplitude given in Eq. (9) of the main text. In the main text, it was argued that the trapping mode of the cavity can be effectively considered as a mechanical potential in the limit of small ζ. We consider the situation where the trapping beam intensity is varied to produce a sinusoidal component in the mechanical spring constant at frequency $2\omega_m$, with an effective Hamiltonian for the motion given by

$$\begin{aligned} H_m &= \frac{\hat{p}^2}{2m} + \frac{1}{2} m \omega_m^2 \hat{x}^2 (1 + 2\epsilon_m \sin\, 2\omega_m t) && \text{(G1)} \\ &= \hbar \omega_m \hat{b}^\dagger \hat{b} - i \frac{\hbar \beta}{2} (\hat{b}^2 e^{2i\omega_m t} - {\hat{b}^\dagger}^2 e^{-2i\omega_m t}) + 2 \left\{ \hbar \beta \hat{b}^\dagger \hat{b} \sin\, 2\omega_m t \right\}. && \text{(G2)} \end{aligned}$$

In the last line, we have re-written $\hat{x} = \sqrt{\frac{\hbar}{2m\omega_m}}(\hat{b} + \hat{b}^\dagger)$ and $\hat{p} = i\sqrt{\frac{\hbar m \omega_m}{2}}(\hat{b}^\dagger - \hat{b})$ in terms of the harmonic oscillator annihilation operator $\hat{b}$ and also defined $\beta = \epsilon \omega_m / 2$ (unrelated to the β term defined in the previous section for a NOPA). The term in braces is a fast-varying contribution to the Hamiltonian, in addition to the "ideal" squeezing Hamiltonian comprising the remaining terms. The external Hamiltonian H_e (see Eq. (6) in the main text) in this case is

$$H_e = -i \frac{\hbar \beta}{2} (\hat{b}^2 e^{2i\omega_m t} - {\hat{b}^\dagger}^2 e^{-2i\omega_m t}) + 2\hbar \beta \hat{b}^\dagger \hat{b} \sin\, 2\omega_m t, \tag{G3}$$

while the Heisenberg equations of motion read

$$\begin{aligned}\frac{d}{dt}\hat{a}_2 &= -\frac{\kappa}{2}\hat{a}_2 - i\Omega_m\left(\hat{b}+\hat{b}_2^\dagger e^{2i\omega_m t}\right)+\sqrt{\kappa}\hat{a}_{2,\mathrm{in}},\\ \frac{d}{dt}\hat{b} &= -i\Omega_m\left(\hat{a}_2+\hat{a}_2^\dagger e^{2i\omega_m t}\right)+i\hat{F}(t)e^{i\omega_m t}+\beta\hat{b}^\dagger-2i\beta\hat{b}\sin 2\omega_m t.\end{aligned} \tag{G4}$$

We proceed to solve these equations in the Fourier domain using the same techniques described in Sec. F. Specifically, we truncate terms containing frequency components $\omega+2n\omega_m$ (integer n) at $|n|\geq 2$ and solve for $\hat{a}(\omega),\hat{b}(\omega)$ in terms of $\hat{F}(\omega)$ and $\hat{a}_{\mathrm{in}}(\omega)$, from which any correlation functions for the cavity field or mechanical motion can be obtained. The input field is assumed to be in the vacuum state. Similarly, the properties of the output field can be obtained from these solutions by using the relation $\hat{a}_{\mathrm{out}}=\sqrt{\kappa}\hat{a}-\hat{a}_{\mathrm{in}}$.

We are specifically interested in the properties of the operator $X_{+,\mathrm{out}}(\omega=0)=\hat{a}_{\mathrm{out}}(\omega=0)+\hat{a}_{\mathrm{out}}^\dagger(\omega=0)$. The general solutions of Eq. (G4) in the Fourier domain are quite cumbersome, so we consider the simplified limit where we set $\Gamma=\kappa$, and take the parametric driving strength to be $\beta=\frac{\Gamma}{2}(1-\delta_t)$, where $\delta_t\ll 1$ is a small parameter that characterizes how far one operates from threshold ($\beta\to\Gamma/2$). Expanding to lowest order in κ/ω_m and δ_t and ignoring fast-rotating terms, we find the following variance,

$$\Delta X_{+,\mathrm{out}}^2(\omega=0)\approx\frac{5}{16}\frac{\kappa^2}{\omega_m^2}+\frac{3}{32}\frac{\kappa^2}{\omega_m^2}\delta_t+\frac{2\phi\omega_m}{\kappa}(1+\delta_t)+\frac{\delta_t^2}{4}. \tag{G5}$$

In particular, at threshold ($\delta_t=0$), one recovers Eq. (9) of the main text. Maximum squeezing of the variance on threshold is achieved when $\kappa=2(2\phi/5)^{1/3}\omega_m$, in which case $(\Delta X_{+,\mathrm{out}}^2)_{\min}=(3/2)(5\phi^2/2)^{1/3}$.

Now we consider the effects of cavity loss on the maximum achievable squeezing of output light. Starting from Eq. (9) for the squeezing at threshold in an ideal cavity (with $\Gamma\sim\kappa$), we model cavity losses via a beam splitter transformation with the ideal squeezed light and vacuum as the two inputs. The output light exhibits reduced squeezing due to mixing with the vacuum, given by

$$(\Delta X_{+,\mathrm{out}}^2(\omega=0))_{\min}=\left(1-\frac{\kappa'}{\kappa}\right)\left(\frac{2\phi\omega_m}{\kappa}+\frac{5}{16}\frac{\kappa^2}{\omega_m^2}\right)+\frac{\kappa'}{\kappa}, \tag{G6}$$

where κ',κ denote the scattering/absorption loss in the cavity and the total cavity linewidth, respectively. In the relevant regime where $\kappa'/\kappa\ll 1$, we can approximate $1-\kappa'/\kappa\approx 1$ and the squeezing is optimized for the choice $\kappa=2(2/5)^{1/3}(\phi+\kappa'/(2\omega_m))^{1/3}$, for which

$(\Delta X^2_{+,\mathrm{out}})_{\mathrm{min}} \approx 2.04(\phi + \kappa'/(2\omega_m))^{2/3}$. We now must choose a set of realistic cavity parameters where this optimized squeezing can be realized, and where $\Gamma \sim \kappa$ is consistent with ζ being small. As an example, taking a cavity length and waist of $L \sim 2$ cm and $w \sim 10$ μm, κ' corresponding to 1 ppm losses per round trip, and sphere parameters $r \sim 35$ nm and $\omega_m/(2\pi) \sim 0.65$ MHz, we find that $\Gamma \sim \kappa$ corresponds to a value $\zeta \sim 1/4$, which yields squeezing of $\sim$15 dB in the output light.

Thus far, we have neglected to consider corrections due to a possibly large position uncertainty Δx for the CM motion of the sphere. Specifically, as one approaches threshold, one quadrature of motion becomes infinitely unsqueezed, producing a large Δx. At the same time, faithful quantum state transfer requires a linear opto-mechanical coupling, where $\mathcal{O}(x^2)$ shifts in the cavity cooling mode frequency can be ignored. Specifically, the Lamb-Dicke parameter $\eta \equiv k\Delta x \ll 1$ for the trapped sphere must remain small. To quantify this effect, we consider the situation where we operate away from threshold by an amount that decreases the squeezing by just 1 dB relative to $(\Delta X^2_{+,\mathrm{out}})_{\mathrm{min}}$. The value of δ_t corresponding to this 1 dB increase can be obtained by solving Eq. (G5), and plugged into the solutions of Eq. (G4) to numerically find Δx. For concreteness, here we associate Δx with the position uncertainty in the unsqueezed quadrature of motion. The corresponding Lamb-Dicke parameter as a function of sphere size is then plotted in Fig. 6 for the choice $\omega_m/(2\pi) = 1$ MHz, and it is seen that $\eta < 10^{-2}$ over the entire parameter regime.

[1] Cleland, A. Optomechanics: Photons refrigerating phonons. *Nature Phys.* **5**, 458–460 (2009).

[2] Mamin, H. J. & Rugar, D. Sub-attonewton force detection at millikelvin temperatures. *Appl. Phys. Lett.* **79**, 3358–3360 (2001).

[3] Cleland, A. N. & Geller, M. R. Superconducting Qubit Storage and Entanglement with Nanomechanical Resonators. *Phys. Rev. Lett.* **93**, 070501 (2004).

[4] Hao, Z., Erbil, A. & Ayazi, F. An analytical model for support loss in micromachined beam resonators with in-plane flexural vibrations. *Sens. Actuators A* **109**, 156 – 164 (2003).

[5] Lifshitz, R. & Roukes, M. L. Thermoelastic damping in micro- and nanomechanical systems. *Phys. Rev. B* **61**, 5600–5609 (2000).

[6] Ashkin, A. *Optical Trapping and Manipulation of Neutral Particles Using Lasers: a Reprint*

Volume with Commentaires (World Scientific, 2007).

[7] Ashkin, A. & Dziedzic, J. M. Optical levitation in high vacuum. *Appl. Phys. Lett.* **28**, 333–335 (1976).

[8] Libbrecht, K. G. & Black, E. D. Toward quantum-limited position measurements using optically levitated microspheres. *Phys. Lett. A* **321**, 99–102 (2004).

[9] Braginsky, V. B. & Vyatchanin, S. P. Low quantum noise tranquilizer for Fabry-Perot interferometer. *Phys. Lett. A* **293**, 228–234 (2002).

[10] Wilson-Rae, I., Nooshi, N., Zwerger, W. & Kippenberg, T. J. Theory of Ground State Cooling of a Mechanical Oscillator Using Dynamical Backaction. *Phys. Rev. Lett.* **99**, 093901 (2007).

[11] Marquardt, F., Chen, J. P., Clerk, A. A. & Girvin, S. M. Quantum Theory of Cavity-Assisted Sideband Cooling of Mechanical Motion. *Phys. Rev. Lett.* **99**, 093902 (2007).

[12] Zeng, H. & Lin, F. Quantum conversion between the cavity fields and the center-of-mass motion of ions in a quantized trap. *Phys. Rev. A* **50**, R3589–R3592 (1994).

[13] Parkins, A. S. & Kimble, H. J. Quantum state transfer between motion and light. *J. Opt. B* **1**, 496–504 (1999).

[14] Zhang, J., Peng, K. & Braunstein, S. L. Quantum-state transfer from light to macroscopic oscillators. *Phys. Rev. A* **68**, 013808 (2003).

[15] Jähne, K. *et al.* Cavity-assisted squeezing of a mechanical oscillator. *Phys. Rev. A* **79**, 063819 (2009).

[16] Wu, L.-A., Xiao, M. & Kimble, H. J. Squeezed states of light from an optical parametric oscillator. *J. Opt. Soc. Am. B* **4**, 1465–1475 (1987).

[17] Yonezawa, H., Braunstein, S. L. & Furusawa, A. Experimental Demonstration of Quantum Teleportation of Broadband Squeezing. *Phys. Rev. Lett.* **99**, 110503 (2007).

[18] Einstein, A., Podolsky, B. & Rosen, N. Can Quantum-Mechanical Description of Physical Reality Be Considered Complete? *Phys. Rev.* **47**, 777–780 (1935).

[19] McKeever, J. *et al.* State-Insensitive Cooling and Trapping of Single Atoms in an Optical Cavity. *Phys. Rev. Lett.* **90**, 133602 (2003).

[20] Maunz, P. *et al.* Cavity cooling of a single atom. *Nature* **428**, 50–52 (2004).

[21] Leibfried, D., Blatt, R., Monroe, C. & Wineland, D. Quantum dynamics of single trapped ions. *Rev. Mod. Phys.* **75**, 281–324 (2003).

[22] Jost, J. D. *et al.* Entangled mechanical oscillators. *Nature* **459**, 683–685 (2009).

[23] Murch, K. W., Moore, K. L., Gupta, S. & Stamper-Kurn, D. M. Observation of quantum-measurement backaction with an ultracold atomic gas. *Nature Phys.* **4**, 561–564 (2008).

[24] Brennecke, F., Ritter, S., Donner, T. & Esslinger, T. Cavity Optomechanics with a Bose-Einstein Condensate. *Science* **322**, 235–238 (2008).

[25] Zener, C. Non-adiabatic crossing of energy levels. *Proc. R. Soc. London A* 696–702 (1932).

[26] Cirac, J. I., Zoller, P., Kimble, H. J. & Mabuchi, H. Quantum State Transfer and Entanglement Distribution among Distant Nodes in a Quantum Network. *Phys. Rev. Lett.* **78**, 3221–3224 (1997).

[27] Beveratos, A., Brouri, R., Gacoin, T., Poizat, J.-P. & Grangier, P. Nonclassical radiation from diamond nanocrystals. *Phys. Rev. A* **64**, 061802 (2001).

[28] Bahns, J. T., Stwalley, W. C. & Gould, P. L. Laser cooling of molecules: A sequential scheme for rotation, translation, and vibration. *J. Chem. Phys.* **104**, 9689–9697 (1996).

[29] Epstein, P. S. On the Resistance Experienced by Spheres in their Motion through Gases. *Phys. Rev.* **23**, 710–733 (1924).

[30] Wineland, D. J. & Itano, W. M. Laser cooling of atoms. *Phys. Rev. A* **20**, 1521–1540 (1979).

[31] Cirac, J. I., Blatt, R., Zoller, P. & Phillips, W. D. Laser cooling of trapped ions in a standing wave. *Phys. Rev. A* **46**, 2668–2681 (1992).

[32] Kokorowski, D. A., Cronin, A. D., Roberts, T. D. & Pritchard, D. E. From single-to multiple-photon decoherence in an atom interferometer. *Phys. Rev. Lett.* **86**, 2191–2195 (2001).

[33] Gardiner, C. W. & Collett, M. J. Input and output in damped quantum systems: Quantum stochastic differential equations and the master equation. *Phys. Rev. A* **31**, 3761–3774 (1985).

[34] Duan, L.-M., Giedke, G., Cirac, J. I. & Zoller, P. Inseparability Criterion for Continuous Variable Systems. *Phys. Rev. Lett.* **84**, 2722–2725 (2000).

[35] Julsgaard, B., Kozhekin, A. & Polzik, E. S. Experimental long-lived entanglement of two macroscopic objects. *Nature* **413**, 400–403 (2001).

[36] Rugar, D. & Grütter, P. Mechanical parametric amplification and thermomechanical noise squeezing. *Phys. Rev. Lett.* **67**, 699–702 (1991).

[37] Hood, C. J., Kimble, H. J. & Ye, J. Characterization of high-finesse mirrors: Loss, phase shifts, and mode structure in an optical cavity. *Phys. Rev. A* **64**, 033804 (2001).

[38] Venkatathri, N. & Yoo, J. W. Synthesis and Characterizationof Silica Nanosphere from Octadecyltrimethoxy Silane. *Bull. Korean Chem. Soc.* **29**, 29 (2008).

[39] Shu, J. *et al.* Elastic light scattering from nanoparticles by monochromatic vacuum-ultraviolet radiation. *J. Chem. Phys.* **124**, 034707 (2006).

[40] Hackermüller, L., Hornberger, K., Brezger, B., Zeilinger, A. & Arndt, M. Decoherence of matter waves by thermal emission of radiation. *Nature* **427**, 711–714 (2004).

[41] Vahala, K. J. Optical microcavities. *Nature* **424**, 839–846 (2003).

[42] Vučković, J. & Yamamoto, Y. Photonic crystal microcavities for cavity quantum electrodynamics with a single quantum dot. *Appl. Phys. Lett.* **82**, 2374–2376 (2003).

[43] Wineland, D. J. *et al.* Trapped atomic ions and quantum information processing. In Roos, C., Haffner, H. & Blatt, R. (eds.) *Proceedings of the International Conference on Atomic Physics (ICAP 2006)*, 103–110 (American Institute of Physics, 2006).

[44] Rabl, P. *et al.* A quantum spin transducer based on nano electro-mechancial resonator arrays. *ArXiv e-prints* (2009). 0908.0316.

[45] Stratton, J. A. *Electromagnetic theory, 1st ed.* (McGraw-Hill, New York, 1941).

[46] Liu, F., Daun, K. J., Snelling, D. R. & Smallwood, G. J. Heat conduction from a spherical nano-particle: status of modeling heat conduction in laser-induced incandescence. *Appl. Phys. B* **83**, 355–382 (2006).

[47] Lang, M. L. & Wolfe, W. L. Optical constants of fused silica and sapphire from 0.3 to 25 μm. *Appl. Opt.* **22**, 1267–1268 (1983).

[48] Rodriguez, A., Soljacic, M., Joannopoulos, J. D. & Johnson, S. G. $\chi^{(2)}$ and $\chi^{(3)}$ harmonic generation at a critical power in inhomogeneous doubly resonant cavities. *Opt. Express* **15**, 7303–7318 (2007).

[49] Gehm, M. E., O'Hara, K. M., Savard, T. A. & Thomas, J. E. Dynamics of noise-induced heating in atom traps. *Phys. Rev. A* **58**, 3914–3921 (1998).

[50] Klimov, V. V., Ducloy, M. & Letokhov, V. S. Spontaneous emission of an atom placed near a prolate nanospheroid. *Eur. Phys. J. D* **20**, 133–148 (2002).

[51] Volkov, A. N. Aerodynamic coefficients of a spinning sphere in a rarefied-gas flow. *Fluid Dynamics* **44**, 141–157 (2009).

[52] Ou, Z. Y., Pereira, S. F., Kimble, H. J. & Peng, K. C. Realization of the Einstein-Podolsky-Rosen paradox for continuous variables. *Phys. Rev. Lett.* **68**, 3663–3666 (1992).

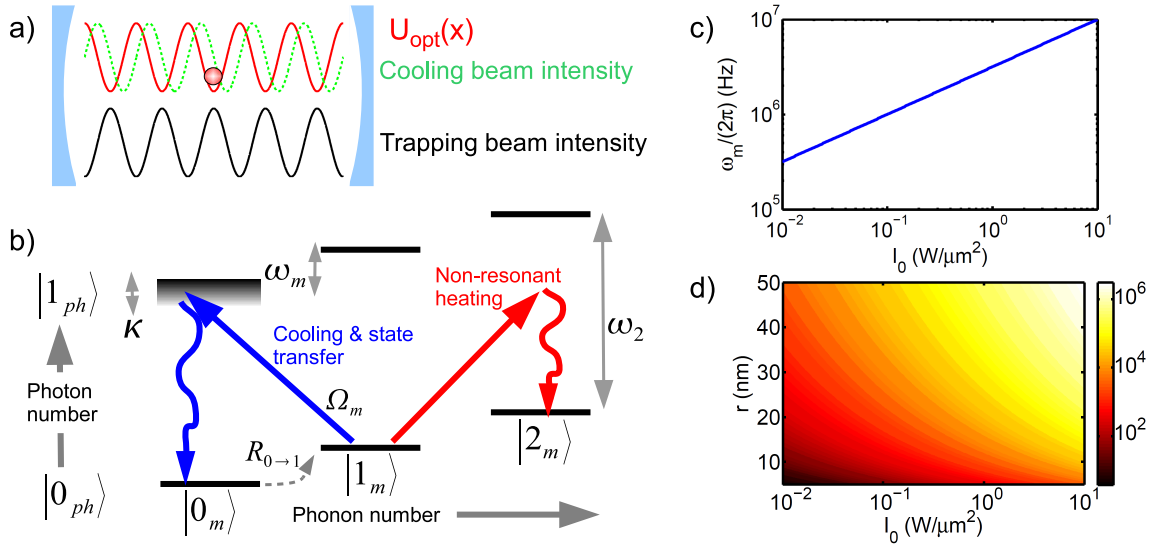

FIG. 1: a) Illustration of dielectric sphere trapped in optical cavity. The large trapping beam intensity provides an optical potential $U_{\rm opt}(x)$ that traps the sphere near an anti-node. A second more weakly driven cavity mode with a non-vanishing intensity gradient at the trap center is used to cool the motion of the sphere. b) Energy level diagram of mechanical motion (denoted m) and cavity cooling mode (ph). The mechanical mode has frequency ω_m, while the optical mode has frequency ω_2 and linewidth κ. Photon recoil induces transitions between mechanical states $|n_m\rangle \rightarrow |(n\pm1)_m\rangle$ at a rate $R_{n\rightarrow n\pm1}$ ($R_{0\rightarrow1}$ shown by dashed gray arrow). The cooling beam, with effective opto-mechanical driving amplitude Ω_m, induces anti-Stokes scattering that cools the mechanical motion and allows for quantum state transfer between motion and light. This beam is also responsible for weaker, off-resonant heating via Stokes scattering. c) Mechanical frequency ω_m as a function of trapping beam intensity. For all numerical results, we take $\lambda = 1$ μm, $\rho = 2$ g/cm^3, and a high index material ($\frac{\epsilon-1}{\epsilon+2}\sim1$). d) Optical trap depth U_0 (in K) as functions of trapping beam intensity and sphere radius r.

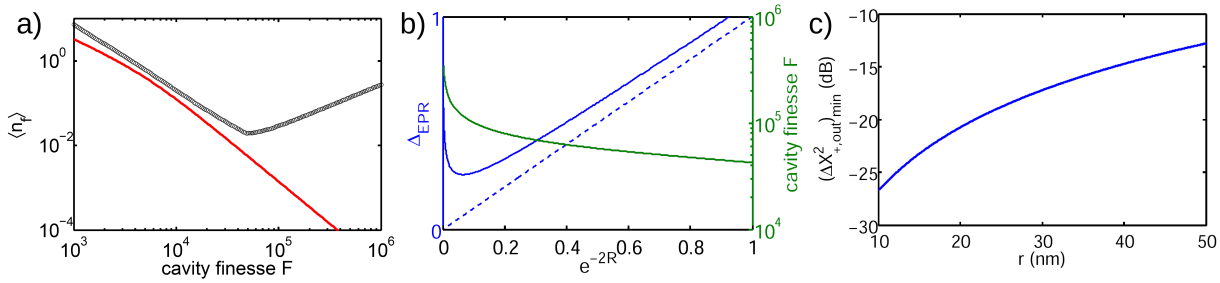

FIG. 2: a) Mean phonon number $\langle n_f \rangle$ (black curve) versus cavity finesse F ($F = \pi c/2\kappa L$) under optimized cooling conditions. The sphere size is $r = 50$ nm and the cavity has a length and waist of $L = 1$ cm, $w = 25$ μm, respectively. The red curve denotes $\tilde{n}_{f,\mathrm{min}}$, the fundamental limit of cooling imposed by sideband resolution. b) Solid blue curve: optimized EPR variance between two levitated spheres, as a function of squeezing parameter e^{-2R}. System parameters are identical to a). Dashed curve: EPR variance in limit of perfect state transfer, $\Delta_{\mathrm{EPR}} = e^{-2R}$. Green curve: cavity finesse corresponding to optimal EPR variance. c) Optimized variance $(\Delta X^2_{+,\mathrm{out}})_{\mathrm{min}}$ (in dB) of squeezed output light from an ideal cavity, as a function of sphere size.

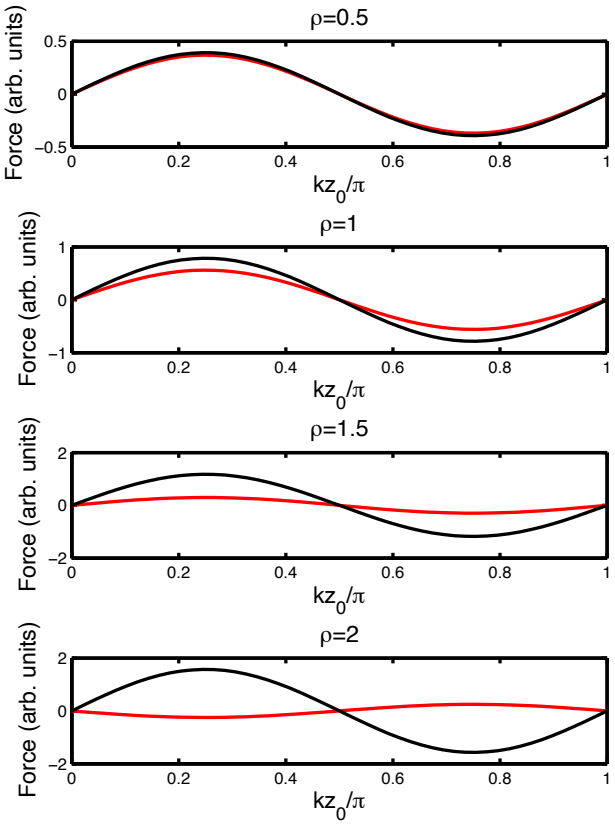

FIG. 3: Comparison of optical forces (in arbitrary units) acting on a dielectric sphere of permittivity $\epsilon = 2$ as a function of position kz_0. The four figures shown correspond to sphere sizes of $\rho \equiv k\sqrt{\epsilon}r = 0.5, 1, 1.5, 2$. The black curve indicates the results obtained from an electrostatic, point-dipole approximation, while the red curve denotes exact electrodynamical theory.

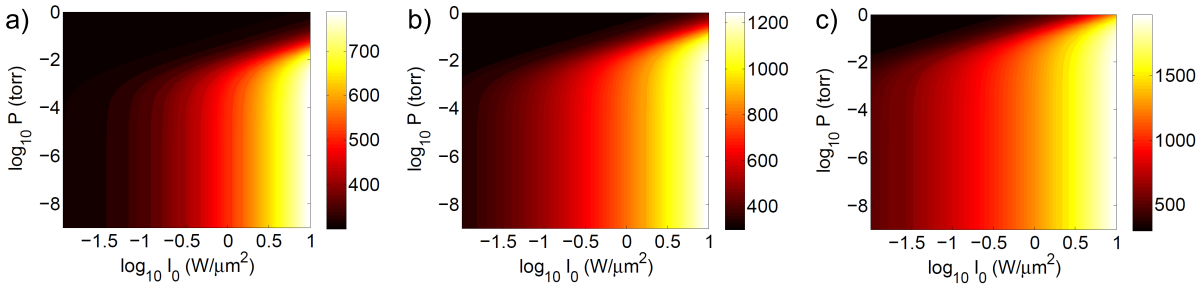

FIG. 4: Internal temperature of sphere (in K), as functions of background gas pressure and intracavity intensity. Material parameters for the sphere are given in the text. Optical losses for the sphere are assumed to be a) 10 dB/km, b) 100 dB/km, and c) 1000 dB/km.

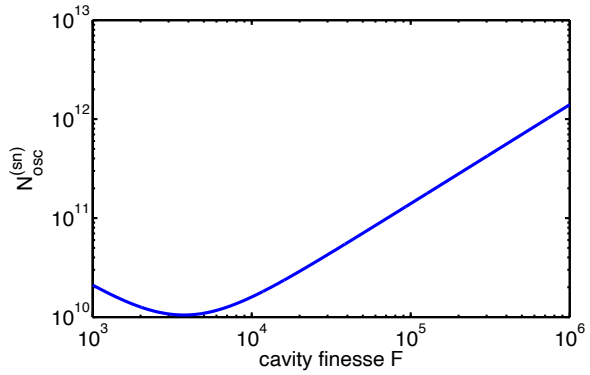

FIG. 5: The number of coherent oscillations $N_{\rm osc}$ allowed before a quantum jump due to shot noise, as a function of cavity finesse. The system parameters are given in the text.

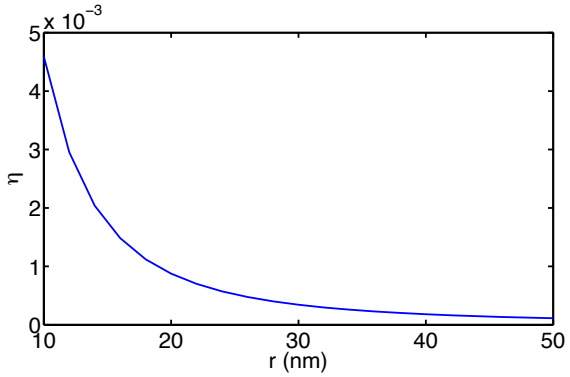

FIG. 6: The Lamb-Dicke parameter $\eta = k\Delta x$ corresponding to the squeezed motional state of the sphere, as a function of sphere size. The squeezing parameters are chosen such that the squeezing in the output light is increased by 1 dB over $(\Delta X^2_{+,\mathrm{out}})_{\mathrm{min}}$. The physical parameters of the system are taken to be $\lambda = 1$ μm, $\rho = 2$ g/cm^3, $\frac{\epsilon-1}{\epsilon+2}\sim 1$, and $\omega_m/(2\pi) = 1$ MHz.